*J. Fluid Mech.* (1974), *vol.* 62, *part* 4, *pp.* 753–773
*Printed in Great Britain*



# Linear stability theory of oscillatory Stokes layers

By CHRISTIAN VON KERCZEK
AND STEPHEN H. DAVIS

Department of Mechanics and Materials Science,
The Johns Hopkins University

(Received 23 July 1973)

The stability of the oscillatory Stokes layers is examined using two quasi-static linear theories and an integration of the full time-dependent linearized disturbance equations. The full theory predicts absolute stability within the investigated range and perhaps for all the Reynolds numbers. A given wavenumber disturbance of a Stokes layer is found to be *more stable* than that of the motionless state (zero Reynolds number). The quasi-static theories predict strong inflexional instabilities. The failure of the quasi-static theories is discussed.

## 1. Introduction

The flow induced in a semi-infinite body of fluid by a harmonically oscillating plate of infinite extent was analysed by Stokes. He found a solution to the constant density Navier–Stokes equations which is a time-periodic plane parallel flow along the wall. This is called the Stokes layer.

Apart from being an *exact* solution of the unsteady Navier–Stokes equations, the Stokes layer plays the role of the prototype viscous boundary-layer correction in 'high frequency' subsonic oscillatory flows. An immediate example is the flow in a pipe driven by a pulsatile pressure gradient. This flow can be analysed by using a Stokes layer on the wall and matching to an inviscid core.

If a closed body, say, a sphere, is oscillated along a diameter, the fluid flow can be analysed using inviscid theory far away. The slip near the body is corrected by a boundary layer (Wang 1965; Riley 1966) which at leading order in oscillation amplitude is a Stokes layer. This modified Stokes layer possesses a normal as well as a tangential velocity component and at second order a steady tangential drift velocity. A similar situation occurs at the bottom of a water channel (Longuet-Higgins 1953) over which a travelling wave propagates.

Dynamic (parametric) stabilization and destabilization of certain flows due to superposed modulation has become a popular subject recently, in large part prompted by the experiments of Donnelly (1964), who modulated the inner cylinder of a concentric cylinder experiment. He found that the modulation at small amplitude could stabilize the Couette flow in that the critical Taylor number for instability was raised. Grosch & Salwen (1968) considered the stability of modulated plane Poiseuille flow using linear theory. They found a stabilization at low modulation amplitude but a destabilization at larger amplitude.

Past work on the stability of oscillatory flows concerns not only the Stokes layer but also the *finite Stokes layers* which have a second (stationary) infinite plate parallel to the first. A simple exact solution of the Navier–Stokes equations is still available. This solution well approximates the Stokes-layer solution for 'large' separation distances.

Conrad & Criminale (1965) first attempted an energy stability theory on one example of a finite Stokes layer. Davis (1971) and von Kerczek & Davis (1972) clarified the interpretation of energy theory for time-dependent flows; the latter computed the energy limit $R_E$ for all separation distances. In the limiting case of the Stokes layer they found that, if $R^\delta \equiv (2U_0^2/\nu\omega)^{\frac{1}{2}} < R_E = 19{\cdot}0$, then disturbances of arbitrary amplitude *decay monotonically and exponentially to zero* as time approaches infinity. If only two-dimensional disturbances are considered, a similar statement holds for $R^\delta < 38{\cdot}9$. Here $U_0$ and $\omega$ are the velocity amplitude and angular frequency of the harmonic wall motion; $\nu$ is the kinematic viscosity of the fluid. Davis & von Kerczek (1973) have reformulated energy theory to allow the possibility that during part of the cycle a disturbance grows but still there is a net exponential decay over a cycle. They computed this new energy limit for all the finite Stokes layers. For the limiting case of the Stokes layer they found that, if $R^\delta < R_{ME}$, then absolute exponential stability is guaranteed. Here $R_{ME}$ is 24·2 for three-dimensional disturbances and 46·6 if only two-dimensional disturbances are allowed.

The only linear-theory stability analysis for Stokes layers is that of Collins (1963). He makes the quasi-static assumption, i.e. the basic flow is assumed to vary so slowly compared with the growth of a disturbance that it can be treated as a steady basic state using an instantaneous 'frozen' profile. He then does a two-dimensional analysis by applying an asymptotic formula for steady boundary layers due to Lin and concludes that the critical Reynolds number $R_L$ of linear theory is 21·4. This value is precluded by the two-dimensional results of the above energy theories. The correct quasi-static $R_L$ for this profile is $R_L = 563$, obtained by direct numerical integration. *One* difficulty in quasi-static theory is the choice of which frozen profile to use. Collins actually uses a very stable one, not that which is most dangerous.

The instability of the Stokes layers is alluded to by Rosenblat (1968) (also see Ffowcs Williams, Rosenblat & Stuart 1969) in his analysis of *inviscid* oscillatory Couette flow. His conclusion is that a velocity–vorticity phase shift is necessary for such an instabilty.

The only experimental work directly on the Stokes-layer instability is that of Li (1954), O'Brien & Logan (1965) and Sergeev (1966). Li examined the layer on an oscillating plate and found using visual means that the critical Reynolds number for transition to turbulence is 566. O'Brien & Logan examined the same situation and were able to attain the Reynolds numbers up to 130. Within this range no instability was apparent. Sergeev examined the flow in a circular tube generated by oscillating bellows. He used both visual means and measurements on the power input to the bellows to assess transition. In a series of nearly 100 experiments, he found a transition Reynolds number of 500 when the flow is well approximated by a Stokes layer near the wall matched to an inviscid core.

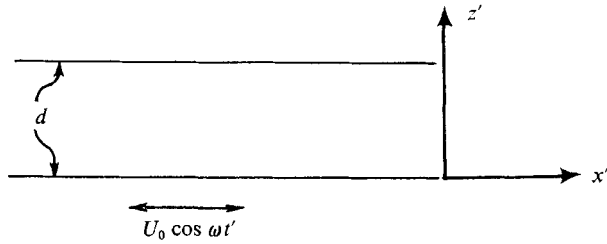


FIGURE 1. The geometry of the finite Stokes layer.

The modified Stokes layer on the bottom of a water channel over which small surface waves travel was examined by Vincent (1957) and Collins (1963) using visual techniques. Transition Reynolds numbers of 113 and 160, respectively, were found.

As has been seen, complicated oscillatory flows can be conveniently analysed by decomposing the flow into two parts: an inviscid outer flow plus a viscous boundary-layer correction. This boundary layer is often of the Stokes type. An attractive possibility is that the *stability* of such complicated flows might be examined by treating the stability of each part separately. The object of the present work is to assess the stability of the Stokes layer according to linear theory. For technical reasons, finite Stokes layers will be examined. Two quasi-static theories and the full time-dependent linear problem will be evaluated and compared. The results will be interpreted in the light of the experiments and in terms of more general flows.

## 2. Formulation

Consider an incompressible Newtonian viscous fluid of constant density $\rho$ and kinematic viscosity $\nu$ confined between two infinite parallel plates a distance $d$ apart (see figure 1). Let $(x', y', z')$ be the Cartesian co-ordinates of a system with its origin in one of the plates, with its $x'$ and $y'$ axes parallel to the plates and with its $z'$ axis normal to the plates. The corresponding velocity vector and pressure are given by $(u', v', w')$ and $p'$. The plate at $z' = 0$ oscillates with the velocity $U_0 \cos \omega t'$ in the $x'$ direction, where $t'$ is the time, $\omega$ is the angular frequency of oscillation and $U_0$ is the velocity amplitude. The plate at $z' = d$ is stationary.

The problem can be scaled by introducing the following non-dimensional variables:

$$t = \omega t', \quad (u, v, w) = U_0^{-1}(u', v', w'), \quad p = \rho \nu U_0 \delta^{-1} p'$$

and

$$(x, y, z) = \delta^{-1}(x', y', z'),$$

where $\delta = (2\nu/\omega)^{\frac{1}{2}}$ is the Stokes length. Two non-dimensional groups emerge: the Stokes–Reynolds number $R^\delta = U_0 \delta / \nu$ and $\beta = d/\delta$.

In terms of these Stokes scales, a *periodic basic solution* for the induced fluid flow is as follows:

$$\mathbf{v}_0 = (\mathscr{U}(z,t), 0, 0), \quad p_0 \equiv 0, \tag{2.1a}$$

where

$$\mathscr{U}(z,t) = \mathrm{Re}\left\{\frac{\sinh(1+i)(\beta - z)}{\sinh(1+i)\beta} e^{it}\right\}. \tag{2.1b}$$

This can be termed a *finite Stokes layer* (von Kerczek & Davis 1972) in analogy with the *Stokes layer* that governs the flow as the stationary plate is removed to infinity:

$$\mathscr{U}(z,t) = e^{-z}\cos(z-t) \quad \text{as} \quad \beta\to\infty. \tag{2.1c}$$

Alternatively, the length $d$ rather than $\delta$ can be used for scaling with the Reynolds number $R^d = U_0 d/\nu$ emerging. On these Reynolds scales, the limiting flow for $\beta\to 0$ has the form

$$\mathscr{U}(\bar{z},t) = (1-\bar{z})\cos t \quad \text{as} \quad \beta\to 0, \tag{2.1d}$$

where $\bar{z} = z/\beta$, and represents modulated plane Couette flow.

## 3. Disturbances

Let the basic state (2.1) be slightly disturbed as follows:

$$\mathbf{v} = \mathbf{v}_0 + \mathbf{v}', \quad p = p_0 + p'.$$

If this disturbed flow is substituted into the governing (non-dimensional) Navier–Stokes and continuity equations (with the primes dropped), then the *linearized* disturbance equations take the form

$$2\partial(u,v,w)/\partial t + R^\delta(w\mathscr{U}_z + \mathscr{U}u_x, \mathscr{U}v_x, \mathscr{U}w_x) = -(p_x,p_y,p_z) + \nabla^2(u,v,w), \tag{3.1a}$$

$$u_x + v_y + w_z = 0. \tag{3.1b}$$

The appropriate boundary conditions are

$$u = v = w = 0 \quad \text{on} \quad z = 0,\beta. \tag{3.1c}$$

Here $\nabla^2$ denotes the Laplacian operator and condition (3.1 $c$) is understood to be taken in the limiting sense $\beta\to\infty$ for the Stokes layer.

Since $\mathscr{U}$ depends on $z$ and $t$ only, the linear system (3.1) can be separated (or Fourier analysed) in $x$ and $y$, and each mode considered separately. Let us define the modes

$$(u,v,w,p) = (\hat{u},\hat{v},\hat{w},\hat{p})\exp[i(\alpha x+\gamma y)],$$

where $\alpha$ and $\gamma$ are *real* wavenumbers (scaled on $\delta$). The system (3.1) then becomes

$$2\partial(\hat{u},\hat{v},\hat{w})/\partial t + R^\delta(\hat{w}\mathscr{U}_z + i\alpha\mathscr{U}\hat{u}, i\alpha\mathscr{U}\hat{v}, i\alpha\mathscr{U}\hat{w}) = -(i\alpha\hat{p}, i\gamma\hat{p}, \hat{p}_z) + \mathscr{L}(\hat{u},\hat{v},\hat{w}), \tag{3.2a,b,c}$$

$$i(\alpha\hat{u}+\gamma\hat{v}) + \hat{w}_z = 0, \tag{3.2d}$$

$$\hat{u} = \hat{v} = \hat{w} = 0 \quad \text{on} \quad z = 0,\beta, \tag{3.2e}$$

where

$$\mathscr{L} = \partial^2/\partial z^2 - (\alpha^2+\gamma^2).$$

## 4. Two- and three-dimensional disturbances

Disturbance waves of general wavenumber $(\alpha,\gamma)$ are called three-dimensional disturbances, whereas those with $\gamma = 0$ are called two-dimensional. In the linear

stability problem of *steady* unidirectional shear flows a transformation can be made (Squire 1933) which reduces the linear stability problem for all three-dimensional disturbances to an equivalent problem for two-dimensional disturbances. An immediate consequence of this transformation is *Squire's theorem*, which states that for every three-dimensional disturbance of wavenumber $(\alpha, \gamma)$ there is a related two-dimensional disturbance with wavenumber $((\alpha^2+\gamma^2)^{\frac{1}{2}}, 0)$ at a *lower* Reynolds number. This relationship is then used to prove that the minimum critical Reynolds number $R_L$ above which at least one disturbance exists that renders the basic state unstable corresponds to a two-dimensional disturbance. *All* three-dimensional disturbances at this and lower Reynolds numbers damp out with time.

Exactly the *same* Squire's theorem can be proved for the Stokes layers and, in fact, any unidirectional unsteady shear flow in which separate time and length scales are defined. (Also see Conrad & Criminale 1965.) The transformation that leads to Squire's theorem for these unsteady flows emerges most readily by considering the flow in terms of variables made dimensionless by the Stokes scales.

For the Stokes layers, multiply (3.2*a*) by $\alpha$, (3.2*b*) by $\gamma$ and add to obtain

$$2(\alpha\hat{u}_t+\gamma\hat{v}_t)+R^\delta(\alpha\hat{w}\mathscr{U}_z+i\alpha^2\mathscr{U}\hat{u}+i\alpha\gamma\hat{v}\mathscr{U}) = -i(\alpha^2+\gamma^2)\hat{p}+\mathscr{L}(\alpha\hat{u}+\gamma\hat{v}). \quad (4.1)$$

Then define

$$\left.\begin{aligned} &\tilde{\alpha}\tilde{u} = \alpha\hat{u}+\gamma\hat{v}, \quad \tilde{p} = \hat{p}, \quad \tilde{w} = \hat{w}, \\ &\tilde{\alpha}^2 = \alpha^2+\gamma^2, \quad \tilde{\alpha}\tilde{R}^\delta = \alpha R^\delta, \end{aligned}\right\} \quad (4.2)$$

and use them in (4.1), (3.2*c*) and (3.2*d*) to obtain

$$2\tilde{u}_t+R^\delta(\tilde{w}\mathscr{U}_z+i\alpha\mathscr{U}\tilde{u}) = -i\tilde{\alpha}\tilde{p}+\mathscr{L}\tilde{u}, \quad (4.3a)$$

$$2\tilde{w}_t+i\tilde{\alpha}\tilde{R}^\delta\mathscr{U}\tilde{w} = -\tilde{p}_z+\mathscr{L}\tilde{w}, \quad (4.3b)$$

$$i\tilde{\alpha}\tilde{u}+\tilde{w}_z = 0, \quad (4.3c)$$

$$\tilde{u} = \tilde{w} = 0, \quad \text{on} \quad z = 0, \beta. \quad (4.3d)$$

Note that problem (4.3) is the same as problem (3.2) with $\gamma = 0$, so that the three-dimensional problem is reduced to an equivalent two-dimensional one. Furthermore, note that there are no changes in $z$ or $t$ and so none in $\mathscr{U}(z,t)$. Hence, any three-dimensional disturbance is related to a two-dimensional one at lower Reynolds number through the relation (4.2). Only two-dimensional disturbances will be examined henceforth.

## 5. The two-dimensional disturbance equation

Let us introduce the disturbance stream function $\phi$ as follows:

$$\hat{u} = \phi_z, \quad \hat{w} = -i\alpha\phi. \quad (5.1)$$

By use of expressions (5.1), and the assumptions $\gamma = \hat{v} \equiv 0$, the system (3.2) can be reduced by cross-differentiation to the following one:

$$2\partial(\mathscr{L}\phi)/\partial t+i\alpha R^\delta(\mathscr{U}\mathscr{L}\phi-\mathscr{U}_{zz}\phi) = \mathscr{L}^2\phi, \quad (5.2a)$$

$$\phi = \phi_z = 0 \quad \text{on} \quad z = 0, \beta. \quad (5.2b)$$

*If* the basic flow were *time-independent*, then normal modes in time could be examined by letting

$$\phi(z,t) = \overline{\phi}(z)\exp\{-i\tfrac{1}{2}\alpha R^{\delta}ct\}. \tag{5.3a}$$

Then, (5.2*a*) becomes

$$(\mathscr{U}-c)\,\mathscr{L}\overline{\phi} - \mathscr{U}_{zz}\overline{\phi} = \frac{1}{i\alpha R^{\delta}}\mathscr{L}^2\overline{\phi}, \tag{5.3b}$$

with

$$\phi = \phi_z = 0 \quad \text{on} \quad z = 0,\beta,$$

when $\mathscr{U}$ is independent of time. This is the classical Orr–Sommerfeld problem.

## 6. A symmetry property

The solutions $\phi(z,t)$ of system (5.2) satisfy the relation

$$\phi(z,t) = \phi^*(z,t-\pi), \tag{6.1}$$

where an asterisk denotes the complex conjugate. This can be proved by noting from (2.1*b*) that $\mathscr{U}(z,t) = -\mathscr{U}(z,t-\pi)$, so that upon taking the complex conjugate of system (5.2) and letting $t = \tau+\pi$, one obtains

$$2\partial(\mathscr{L}\phi^*)/\partial\tau + i\alpha R^{\delta}[\mathscr{U}(z,\tau)\,\mathscr{L}\phi^* - \mathscr{U}_{zz}(z,\tau)\,\phi^*] = \mathscr{L}^2\phi^*,$$

$$\phi^* = \phi_z^* = 0 \quad \text{on} \quad z = 0,\beta.$$

This result is important in the solution of system (5.2) in the following way. Since (5.2) is a linear system with time-periodic coefficients, one expects on the basis of Floquet theory that the solutions can be represented in the form

$$\phi(z,t) = e^{\lambda t}\psi(z,t),$$

where $\psi$ has the same $2\pi$-period as the coefficients if the eigenvalue $\lambda$ is simple. The property (6.1) implies that $\lambda^*$ and $\lambda$ are simultaneous eigenvalues.

Physically, whenever there exists a disturbance wave $\psi(z,t)\exp[\lambda t + i\alpha x]$ that propagates to the right, there is also a wave of the same form propagating to the left. This allows the special case of standing waves, in which $\lambda$ is real. These standing waves would be *synchronous* with the basic state.

Furthermore, the property (6.1) will allow us later in the numerical analysis to infer the solutions for the time interval $[0,2\pi]$ from those for $[0,\pi]$.

## 7. The inviscid limit

In the linear stability theory for *steady* basic states, the inviscid limit $R\to\infty$ of the Orr–Sommerfeld equation (5.3*b*) results in an inviscid problem, one of whose solutions is the proper limit of certain solutions of the Orr–Sommerfeld equation as $R\to\infty$. Hence, the inviscid problem can provide useful information about the instability of the flow. The Rayleigh and Fjørtoft conditions (see Drazin & Howard 1966) necessary for instability are based on the linearized inviscid Orr–Sommerfeld equation. The conditions alert one to certain points of inflexion as candidates for local instability. When these instabilities are present

they have $O(1)$ growth rates. It thus seems natural to inquire as to the inviscid limit of system (5.2).

The basic flow $\mathscr{U}$ is a solution of the (dimensional) diffusion equation

$$(\partial/\partial t' - \nu\,\partial^2/\partial z'^2)\,\mathscr{U} = 0.$$

Hence, the basic flow is *explicitly dependent* on the viscosity coefficient $\nu$. This is in contrast to the steady basic flow normally treated, whose profiles are explicitly independent of $\nu$. In fact, the limit $\nu \to 0$ is not well-defined for the Stokes layers since in this limit the essential balance between local acceleration and viscous forces is destroyed. Only a shear layer at $z = 0$ survives.

As a result, the limiting form of system (5.2) as $\nu \to 0$ is not well defined. Using the Stokes scales, $\beta \to \infty$, and with $\omega^{-1}$ as the time scale, the reduced equation becomes

$$\mathscr{U}\mathscr{L}\phi - \mathscr{U}_{zz}\phi = 0$$

with the Stokes-layer profile (2.1 *c*). Here disturbances are neutral if in fact they are correct inviscid limits of viscous solutions at all.

If, instead of $\omega^{-1}$, the convective time scale $\delta/U_0$ is used, then the $\nu \to 0$ limit of the basic flow is non-uniform in time.

The conclusion is that the inviscid problem no longer plays the role that it did in the stability of *steady* parallel flows. Furthermore, it sounds a warning against inferring instability behaviour on the basis of *instantaneous* points of inflexion.

## 8. Some special limits

Some explicit solutions of problem (5.2) in certain limiting cases can be obtained. These solutions will help in the interpretation of the final results.

Consider the limiting case of $R^\delta \to 0$ with $\beta$ and $\alpha$ fixed. Then (5.2) becomes

$$2\partial(\mathscr{L}\phi)/\partial t = \mathscr{L}^2\phi, \tag{8.1 a}$$

$$\phi = \phi_z = 0 \quad \text{on} \quad z = 0, \beta. \tag{8.1 b}$$

Since the time-dependent basic state is absent, let $\phi = \eta\, e^{-\lambda t}$ and $\zeta = (2/\beta)z - 1$. System (8.1) then becomes

$$L^2\eta + \mu L\eta = 0, \tag{8.2}$$

where $$L = d^2/d\zeta^2 - \xi^2, \quad \xi^2 = \tfrac{1}{4}\beta^2\alpha^2, \quad \mu = \tfrac{1}{2}\lambda\beta^2.$$

The solutions of problem (8.2) are the Dolph–Lewis eigenfunctions (Dolph & Lewis 1958) corresponding to the eigenvalues $\mu_n = u_n^2 + \xi^2$, $n = 1, 2, \ldots$, where the $\xi$ satisfy the transcendental equations

$$u_n \cosh\xi \sin u_n + \xi \sinh\xi \cos u_n = 0 \tag{8.3}$$

or

$$u_n \sinh\xi \cos u_n - \xi \cosh\xi \sin u_n = 0. \tag{8.4}$$

The smallest eigenvalue $\mu_n$ is the first zero of (8.3) and is obtained from the series (Dolph & Lewis 1958) for small $\alpha\beta$:

$$u_1 = \pi + \frac{a}{\pi} - \frac{a^2}{\pi^3} + 2\frac{a^3}{\pi^5} + \ldots,$$

where $a = -\xi \tanh \xi$. From this, the decay rate of disturbances can be obtained:

$$\lambda = \frac{2}{\beta^2}\left[\tfrac{1}{4}\beta^2\alpha^2 + \left(\pi + \frac{a}{\pi} - \frac{a^2}{\pi^3} + 2\frac{a^3}{\pi^5} + \ldots\right)^2\right]. \tag{8.5}$$

Consider the limiting case of $\alpha \to 0$ with $R^\delta$ and $\beta$ fixed. In this limit (5.2) reduces to

$$2\partial\phi_{zz}/\partial t = \phi_{zzzz},$$

$$\phi = \phi_z = 0 \quad \text{on} \quad z = 0, \beta.$$

This is the same problem as (8.2) with $\alpha = 0$, so that the decay rates of these disturbances are immediately obtained from (8.5) as

$$\lambda = 2\pi^2/\beta^2. \tag{8.6}$$

## 9. The Galerkin equation

Consider the class of functions $\{\phi_n(z)\}$ that satisfy $\phi_n = \phi_n' = 0$ on $z = 0, \beta$, have continuous fourth derivatives and are complete in an appropriate sense (von Kerczek 1973). These functions will be used to represent the solution $\phi(z,t)$ of system (5.2) through Galerkin's method.

Assume that we can write

$$\phi(z,t) = \sum_{n=1}^{N} a_n(t)\,\phi_n(z), \tag{9.1}$$

where convergence is presumed as $N \to \infty$. The $N$-term truncated form (9.1) is not an exact solution of (5.2) but if the error is made orthogonal to each $\phi_n$, then the optimal such approximation is obtained. If this is done, then the following system of ordinary differential equations for the amplitude coefficients is obtained:

$$2\hat{\mathbf{Q}}\,d\mathbf{a}/dt = \hat{\mathbf{P}}\mathbf{a} - i\alpha R^\delta \hat{\mathbf{V}}(t)\,\mathbf{a}, \tag{9.2}$$

where

$$\hat{Q}_{mn} = \langle \mathscr{L}\phi_n, \phi_m\rangle, \quad \hat{P}_{mn} = \langle \mathscr{L}^2\phi_n, \phi_m\rangle,$$

$$\hat{V}_{mn}(t) = \langle \mathscr{U}\mathscr{L}\phi_n - \mathscr{U}_{zz}\phi_n, \phi_m\rangle = \hat{C}_{mn}\cos t + \hat{S}_{mn}\sin t,$$

$$\langle a, b\rangle \equiv \int_0^\beta abdz.$$

The matrices $\hat{\mathbf{P}}$ and $-\hat{\mathbf{Q}}$ are symmetric and positive definite. The matrices $\hat{\mathbf{P}}$, $\hat{\mathbf{Q}}$, $\hat{\mathbf{C}}$ and $\hat{\mathbf{S}}$ are all constant. The matrix $\hat{\mathbf{Q}}$ can be inverted to yield the system equivalent to (9.2):

$$2d\mathbf{a}/dt = \mathbf{P}\mathbf{a} - i\alpha R^\delta \mathbf{V}(t)\,\mathbf{a}. \tag{9.3a}$$

It will be convenient to use the shorthand notation

$$\mathbf{A}(t) = \tfrac{1}{2}[\mathbf{P} - i\alpha R^\delta \mathbf{V}(t)], \tag{9.3b}$$

so that the Galerkin equation is then

$$d\mathbf{a}/dt = \mathbf{A}(t)\,\mathbf{a}. \tag{9.3c}$$

## 10. The quasi-static problems

A popular assumption made in treating the stability of time-dependent states is that of quasi-steadiness. There, it is assumed that the scale of variation of a growing or decaying disturbance is much faster than that of the variation of the basic state. If this were so, then the rapidly varying disturbance would to a good approximation feel the effect of only an instantaneous basic state profile. Hence, it would be reasonable to replace the time $t$ in the coefficients of (5.2) by a constant $t_0$ and treat this frozen profile as though it were steady. Since the time has been removed from the coefficients, normal modes in time (5.3*a*) could be used and (5.2) would reduce to the Orr–Sommerfeld equation (5.3*b*). Not only does this procedure avoid the necessity of solving a partial differential equation but it also makes the inviscid limit of the equation well-behaved. In effect, it fixes $\bar{t}/R^\delta$ as $R^\delta \to \infty$, where $\bar{t}$ is a non-dimensional time scaled on the convective time $\delta/U_0$. This non-uniformity in the time-dependent problem was mentioned in §8.

The quasi-static Galerkin system corresponding to (9.3) has constant coefficients. It is then possible to write

$$\mathbf{a}(t;t_0) = \bar{\mathbf{a}}(t_0)\, e^{\lambda(t_0)t}$$

and so the Galerkin system can be solved by obtaining the eigenvalues $\lambda$ of an $N \times N$ matrix,

$$\det(\mathbf{A}(t_0) - \lambda \mathbf{I}) = 0. \tag{10.1}$$

One difficulty involved is the choice of $t_0$, $0 \leqslant t_0 < 2\pi$. In practice, two quasi-static stability criteria are often used.

*Quasi-static theory A*. Find that profile (and hence the corresponding $t_0$) which is most unstable. For that profile, find the smallest positive value of $R^\delta$ (call it $R^\delta_A$) that makes the principal eigenvalue $\lambda_1$ have zero real part. (All other $\lambda_i$'s have negative real part.)

*Quasi-static theory B*. Compute, for a fixed $R^\delta$, $\lambda_1(t_0)$, i.e. find the principal eigenvalue $\lambda_1$ for each $t_0$, $0 \leqslant t_0 < 2\pi$. Then compute

$$\sigma_1(R^\delta) = \int_0^{2\pi} \lambda_1(t_0)\, dt_0.$$

Interpolate on $R^\delta$ to find the smallest positive $R^\delta$ (call it $R^\delta_B$) such that

$$\sigma_1(R^\delta_B) = 0.$$

The analyses of Collins (1963) and Obremski & Morkovin (1969) incorporate approximations respectively similar to types $A$ and $B$.

## 11. The time-dependent problem

The fundamental matrix $\mathbf{F}(t)$ of the $N$-dimensional time-dependent Galerkin equation (9.3) can be represented using the Floquet theorem (Coddington & Levinson 1955, p. 78):

$$\mathbf{F}(t) = \mathbf{B}(t)\, e^{t\mathbf{C}}, \tag{11.1}$$

where $\mathbf{B}$ is a $2\pi$-periodic matrix in $t$ since the basic state is, $\mathbf{C}$ is a constant matrix and the initial value of $\mathbf{F}$ can be taken, without loss of generality, to be the identity matrix:

$$\mathbf{F}(0) = \mathbf{I}. \tag{11.2}$$

Since $\mathbf{B}(t) = \mathbf{B}(t+2\pi)$, it follows from (11.2) that

$$\mathbf{F}(2\pi) = e^{2\pi\mathbf{C}}. \tag{11.3}$$

Since $\mathbf{F}(2\pi)$ is transformed to triangular form and $\mathbf{C}$ to Jordan canonical form by the same transformation matrix, say, $\mathbf{S}$, then the eigenvalues $\lambda$ (called Floquet exponents) of $\mathbf{C}$ are obtained from the eigenvalues $\mu$ of $\mathbf{F}(2\pi)$ by

$$\lambda = (2\pi)^{-1} \ln \mu \pmod{n}. \tag{11.4}$$

*Instability criterion.* Let $\lambda_1$ be the Floquet exponent with the largest real part. If $\operatorname{Re} \lambda_1 \neq 0$, then the Stokes layer is unstable or stable to infinitesimal disturbances according as $\operatorname{Re} \lambda_1 > 0$ or $\operatorname{Re} \lambda_1 < 0$ respectively. If $\operatorname{Re} \lambda_1 = 0$, and if $\lambda_1$ has multiplicity greater than one, then the Stokes layer is unstable.

The criterion necessitates the calculation of the fundamental matrix $\mathbf{F}(t)$ of (9.3). The associated eigenvectors are calculated as follows. Let $\mathbf{S}$ be the matrix that transforms $\mathbf{C}$ to its Jordan canonical form $\mathbf{J}$. Then the fundamental matrix $\mathbf{F}$ becomes transformed to $\mathbf{G}(t)$:

$$\mathbf{G}(t) = \mathbf{F}(t)\,\mathbf{S} = \mathbf{B}(t)\,\mathbf{S}\,e^{(t\mathbf{J})}.$$

The principal eigenvector $\mathbf{a}^{(1)}$ can then be calculated by integrating (9.3) starting with the initial condition

$$\mathbf{a}^{(1)}(0) = e^{-2\pi\lambda_1}\,\mathbf{g}_1(2\pi), \tag{11.5}$$

where $\mathbf{g}_1(2\pi)$ is the associated column vector of $\mathbf{G}(2\pi)$.

The energy transfer operative in the system can be examined by computing the entries in the disturbance energy balance:

$$K = \int_{\mathscr{V}} \tfrac{1}{2}|\mathbf{v}|^2 = -\mathbf{a}^{*T}\hat{\mathbf{Q}}\mathbf{a}, \tag{11.6a}$$

$$\mathscr{D} = \int_{\mathscr{V}} |\nabla \mathbf{v}|^2 = \mathbf{a}^{*T}\hat{\mathbf{P}}\mathbf{a}, \tag{11.6b}$$

$$I(t) = \int_{\mathscr{V}} -uw\mathscr{U}_z(z,t) = -i\alpha\mathbf{a}^{*T}\hat{\mathbf{V}}(t)\,\mathbf{a}. \tag{11.6c}$$

The volume $\mathscr{V}$ covers $0 \leqslant z \leqslant \beta$ and one period in $x$. These are related through the equation

$$2dK/dt = -\mathscr{D} + R^{\delta} I(t). \tag{11.6d}$$

The production term $\Sigma(z)$ *averaged over one period in time* is given by

$$\Sigma(z) = \frac{1}{2\pi}\int_0^{2\pi} \overline{(-uw)}\,\mathscr{U}_z\,dt, \tag{11.7}$$

where the bar denotes an $x$ average over one cycle.

*The symmetry property*

The symmetry property of § 6 translates to the Galerkin system and serves as an aid in the numerical work.

The property becomes $\mathbf{F}(t) = \mathbf{F}^*(t-\pi)$. The fundamental matrix

$$\mathbf{F}(t) \quad (\mathbf{F}(0) = \mathbf{I})$$

is defined for $0 \leqslant t \leqslant 2\pi$. Using the symmetry property, the values of $\mathbf{F}$ on $[\pi, 2\pi]$ can be inferred from those on $[0, \pi]$. Define $\mathbf{F}_1(t)$ such that

$$\mathbf{F}_1(\pi) = \mathbf{I} \quad (\pi \leqslant t \leqslant 2\pi).$$

Then
$$\mathbf{F}(t) = \mathbf{F}_1(t)\,\mathbf{F}(\pi) \quad (\pi \leqslant t \leqslant 2\pi).$$

However, the symmetry property gives

$$\mathbf{F}_1(t) = \mathbf{F}^*(\tau), \quad \tau \in [0, \pi],$$

so
$$\mathbf{F}_1(2\pi) = \mathbf{F}^*(\pi) \quad \text{and} \quad \mathbf{F}(2\pi) = \mathbf{F}^*(\pi)\,\mathbf{F}(\pi). \tag{11.8}$$

Hence, the system (9.3) need be integrated only over $0 \leqslant t \leqslant \pi$.

*A numerical check*

A useful check on the numerical integration can be obtained from the formula

$$\det \mathbf{F}(2\pi) = \prod_{i=1}^{N} \mu_i = \exp\left[\int_0^{2\pi} \operatorname{tr} \mathbf{A}(s)\, ds\right]. \tag{11.9}$$

Here det denotes determinant and tr denotes trace (Coddington & Levinson 1955, p. 82).

Since, from (11.4), $\mu_i = e^{2\pi\lambda_i} \quad (i = 1, 2, \ldots, N)$,

then (11.9) becomes
$$\sum_{i=1}^{N} \lambda_i = \frac{1}{2\pi}\int_0^{2\pi} \operatorname{tr} \mathbf{A}(s)\, ds. \tag{11.10}$$

From the form of the matrix $\mathbf{A}$, it is easy to see that

$$\frac{1}{2\pi}\int_0^{2\pi} \operatorname{tr} \mathbf{A}(s)\, ds = \operatorname{tr}(\tfrac{1}{2}\mathbf{P}), \tag{11.11}$$

so that (11.10) and (11.11) combine to yield

$$\sum_{i=1}^{N} \lambda_i = \tfrac{1}{2} \operatorname{tr} \mathbf{P}. \tag{11.12}$$

The eigenvalues are already known to be either real or complex conjugates and $\mathbf{P}$ is real. This is a strong check since condition (11.12) is independent of $R^\delta$.

## 12. Numerical analysis

*Step* 1. The functions $\{\phi_n(z)\}$ used in the Galerkin procedure are the 'beam' functions $\{f_n(\zeta) | 0 \leqslant \zeta \leqslant 1\}$ scaled to the interval $0 \leqslant z \leqslant \beta$:

$$(d^4/d\zeta^4 - \mu_n^4) f_n = 0, \quad f_n = df_n/d\zeta = 0 \quad \text{on} \quad \zeta = 0, 1. \tag{12.1}$$

The eigenfunctions involve elementary functions (Gallagher & Mercer 1962) and the corresponding eigenvalues $\mu_n$ are zeros of the equation

$$\cosh\mu_n \cos\mu_n - 1 = 0 \quad (n = 1, 2, \ldots),$$

and are to a good approximation (this approximation is accurate to better than 16 significant figures for $n > 12$)

$$\mu_n \doteq \tfrac{1}{2}(2n+1)\pi \quad (n = 1, 2, \ldots).$$

The $\mu_n$ are tabulated in von Kerczek (1973) to 16 significant figures for $1 \leqslant n \leqslant 12$.

The matrices $\hat{\mathbf{Q}}$, $\hat{\mathbf{P}}$ and $\hat{\mathbf{V}}$ are then evaluated by using certain inherent symmetries so that all the matrix entries reduce to algebraic evaluations (von Kerczek 1973).

*Step* 2. The matrix $\hat{\mathbf{Q}}$ was inverted using the subroutine called MINV from the IBM Scientific Subroutine Package. This program uses Gauss–Jordan elimination with complete pivoting (Isaacson & Keller 1966, p. 50). The matrix products $\hat{\mathbf{Q}}^{-1}\hat{\mathbf{P}}$ and $\hat{\mathbf{Q}}^{-1}\hat{\mathbf{V}}$ were then evaluated. The matrix $\mathbf{A}(t)$ is now in hand.

*Step* 3. For the quasi-static problems, the normal modes (5.3*a*) can eliminate the time dependence of the disturbances, so that the eigenvalue $c = c_R + ic_I$ can be evaluated as an eigenvalue of the matrix $\mathbf{A}$. The LR algorithm (Wilkinson & Reinsch 1971, p. 396) was used for this.

*Step* 4. For the full time-dependent problem, the fundamental matrix $\mathbf{F}(t)$ at $t = \pi$ was obtained numerically. The governing Galerkin equation has the form

$$\dot{\mathbf{F}} = \mathbf{A}(t)\,\mathbf{F}, \quad \mathbf{F}(0) = \mathbf{I}. \tag{12.2}$$

A single-step method involving higher derivatives of (12.2) was used. This is a special case of the methods considered by Lambert & Mitchell (1962).

If

$$\mathbf{F}_n \equiv \mathbf{F}(n\Delta t), \quad \mathbf{A}_n \equiv \mathbf{A}(n\Delta t) \quad (n = 0, 1, 2, \ldots),$$

then either of two *implicit* formulae is used: the fourth-order equation

$$\mathbf{F}_{n+1} = \mathbf{F}_n + \tfrac{1}{2}h(\dot{\mathbf{F}}_{n+1} + \dot{\mathbf{F}}_n) + \tfrac{1}{12}h^2(-\ddot{\mathbf{F}}_{n+1} + \ddot{\mathbf{F}}_n) - \tfrac{1}{720}h^5\mathbf{F}^{(\mathrm{v})}(\xi) \tag{12.3a}$$

or the sixth-order one

$$\mathbf{F}_{n+1} = \mathbf{F}_n + \tfrac{1}{2}h(\dot{\mathbf{F}}_{n+1} + \dot{\mathbf{F}}_n) + \tfrac{1}{10}h^2(-\ddot{\mathbf{F}}_{n+1} + \ddot{\mathbf{F}}_n) + \tfrac{1}{120}h^3(\dddot{\mathbf{F}}_{n+1} + \dddot{\mathbf{F}}_n) + \tfrac{1}{100800}h^7\mathbf{F}^{(\mathrm{vii})}(\xi), \tag{12.3b}$$

where $h = \Delta t$ is a step size and $\xi$ a mean value constant. The truncation errors are discussed in von Kerczek (1973). The derivatives of (12.2) can be taken directly:

$$\ddot{\mathbf{F}} = (\mathbf{A}^2 + \dot{\mathbf{A}})\,\mathbf{F} \equiv \mathbf{B}\mathbf{F},$$

$$\dddot{\mathbf{F}} = (\ddot{\mathbf{A}} + 2\dot{\mathbf{A}}\mathbf{A} + \mathbf{A}\mathbf{B})\,\mathbf{F}.$$

The formulae (12.3) can then be written in the form

$$\mathbf{C}_{n+1}\mathbf{F}_{n+1} = \mathbf{D}_n\mathbf{F}_n. \tag{12.4}$$

Hence, at each step,

$$\mathbf{F}_{n+1} = \mathbf{C}_{n+1}^{-1}\mathbf{D}_n\mathbf{F}_n.$$

Hence, the *whole fundamental solution matrix* is found at each step. The relative merits of such a procedure are discussed in von Kerczek & Davis (1974).

For the system (12.3*a*),

$$\mathbf{C}_{n+1} = \mathbf{I} - \tfrac{1}{2}h\mathbf{A}_{n+1} + \tfrac{1}{12}h^2\mathbf{B}_{n+1},$$

$$\mathbf{D}_n = \mathbf{I} + \tfrac{1}{2}h\mathbf{A}_n + \tfrac{1}{12}h^2\mathbf{B}_n.$$

For the system (12.3*b*),

$$\mathbf{C}_{n+1} = \mathbf{I} - \tfrac{1}{2}h\mathbf{A}_{n+1} + \tfrac{1}{10}h^2\mathbf{B}_{n+1} - \tfrac{1}{120}h^3(\ddot{\mathbf{A}}_{n+1} + 2\dot{\mathbf{A}}_{n+1}\mathbf{A}_{n+1} + \mathbf{A}_{n+1}\mathbf{B}_{n+1}),$$

$$\mathbf{D}_n = \mathbf{I} + \tfrac{1}{2}h\mathbf{A}_n + \tfrac{1}{10}h^2\mathbf{B}_n + \tfrac{1}{120}h^3(\ddot{\mathbf{A}}_n + 2\dot{\mathbf{A}}_n\mathbf{A}_n + \mathbf{A}_n\mathbf{B}_n).$$

*Step* 5. From the numerical determination of $\mathbf{F}(\pi)$, the principal eigenvalue $\lambda_1$ was determined through (11.4) from the $\mu$ closest to unity. The eigenvalues $\mu$ of $\mathbf{F}(2\pi)$ were calculated using the LR algorithm.

*Step* 6. When the principal eigenfunction was to be determined, the first entry was normalized to unity and then the LU algorithm (Gaussian elimination; Isaacson & Keller 1966, p. 29) was used to find the remaining components. The procedure is valid here because in *all cases* $\lambda_1$ turned out to be a simple eigenvalue and its associated eigenvector $\mathbf{f}^{(1)}(2\pi)$ has a non-zero first component. The LU algorithm would indicate a singular matrix if this first component were zero. This yields the eigenvector $\mathbf{f}^{(1)}(2\pi)$ associated with $\lambda_1$.

*Step* 7. The initial value $\mathbf{a}^{(1)}(0)$ of the eigenfunction can be obtained from

$$\mathbf{a}^{(1)}(0) = e^{-2\pi\lambda_1}\,\mathbf{f}^{(1)}(2\pi).$$

Given this initial value that generates the principal eigenvector, the system (9.3) is integrated using a fifth-order Runge–Kutta–Nystrom algorithm (Lapidus & Seinfeld 1971, p. 50) as an independent check. At each step, each term of the energy integral equation (11.6*d*), the total energy (11.6*a*) and the production integral (11.7) are evaluated.

An extensive series of checks on the numerical work was made in order to verify the proper functioning of the program and estimate the accuracy of the results. These checks are described in detail by von Kerczek (1973). We mention here only two of them. The first makes use of formula (11.12). For example in the case where $\beta = 8{\cdot}0$, $\alpha = 0{\cdot}5$, $R^\delta = 400$ and $N = 5$, $\frac{1}{2}\operatorname{tr}\mathbf{P} = -7{\cdot}06236$. The sum of the Floquet exponents obtained by integrating system (9.3) using algorithms (12.3*a*, *b*) on 200 equal steps in the interval $[0, \pi]$ on the CDC 6600 computer (14 decimal digit mantissa) are $-7{\cdot}06189$ and $-7{\cdot}06235$ respectively. A similar integration using the Runge–Kutta–Nystrom method on 200 equal time steps and the same machine yielded

$$\sum_{i=1}^{5} \lambda_i = -7{\cdot}05922.$$

The second check involves integrating system (9.3) under the initial condition (11.5). This integration should yield $\mathbf{a}^{(1)}(2\pi) = \mathbf{a}^{(1)}(0)\,e^{2\pi\lambda_1}$ at $t = 2\pi$. Thus, a comparison of $\mathbf{a}^{(1)}(0)$ and $\mathbf{a}^{(1)}(2\pi)$ gives a good consistency and accuracy test of the method. An example of such a calculation is shown in table 1 for the case

| | Real part | | Imaginary part | |
|---|---|---|---|---|
| $h$ | Initial | Final | Initial | Final |
| 1 | 1·0000 | 1·0017 | 0·0 | −1·5193–3 |
| 2 | −1·0295 | −1·0307 | 2·8478–1 | 2·8706–1 |
| 3 | 4·9205–1 | 4·9200–1 | −4·7648–1 | −4·7837–1 |
| 4 | 2·1409–2 | 2·2024–2 | 2·0846–1 | 2·0893–1 |
| 5 | −1·4810–1 | −1·4840–1 | 6·8253–2 | 6·8624–2 |
| 6 | 6·8617–3 | 6·7347–3 | −8·4168–2 | −8·4387–2 |
| 7 | 3·3704–2 | 3·3823–2 | 1·0112–2 | 1·0086–2 |
| 8 | 1·0652–2 | 1·0696–2 | 2·0559–2 | 2·0600–2 |
| 9 | −9·0330–3 | −9·0530–3 | 1·3976–3 | 1·4152–3 |
| 10 | 8·7975–4 | 8·6906–4 | −8·1633–3 | −8·1857–3 |
| 11 | 1·4862–3 | 1·4887–3 | −3·0445–3 | −3·0531–3 |
| 12 | 5·6683–4 | 5·6674–4 | −8·4211–4 | −8·4444–4 |
| 13 | −1·6737–3 | −1·6766–3 | 2·5730–4 | 2·6024–4 |
| 14 | −8·7199–4 | −8·7474–4 | −1·6824–4 | −1·6787–4 |
| 15 | −6·6531–4 | −6·6611–4 | 3·2092–4 | 3·2239–4 |
| 16 | 2·8614–5 | 2·8701–5 | 2·3293–4 | 2·3332–4 |
| 17 | −1·5703–5 | −1·5168–5 | 3·4740–4 | 3·4827–4 |
| 18 | 2·1291–4 | 2·1332–4 | 8·6178–5 | 8·6106–5 |
| 19 | 8·9271–5 | 8·9639–5 | 5·7387–5 | 5·7461–5 |
| 20 | 1·5448–4 | 1·5463–4 | −9·1145–5 | −9·1539–5 |
| 21 | 3·4119–5 | 3·4196–5 | −6·3620–5 | −6·3774–5 |
| 22 | 5·7499–5 | 5·7450–5 | −1·1200–4 | −1·1233–4 |
| 23 | −1·4058–5 | −1·4114–5 | −6·2342–5 | −6·2450–5 |
| 24 | 1·5821–5 | 1·5735–5 | −7·4882–5 | −7·5075–5 |
| 25 | −1·7082–5 | −1·7130–5 | 3·3403–5 | −3·3449–5 |
| 26 | 1·2178–5 | 1·2133–5 | −4·0587–5 | −4·0697–5 |

TABLE 1. The initial values of the eigenvector $\mathbf{a}^{(1)}(0)$ corresponding to $\lambda_1$ compared with $\mathbf{a}^{(1)}(2\pi)e^{-2\pi\lambda_1}$. $\beta = 8{\cdot}0$, $\alpha = 0{\cdot}5$, $R^\delta = 600$ and $N = 26$.

$\beta = 8{\cdot}0$, $\alpha = 0{\cdot}5$, $R^\delta = 600$ and $N = 26$. The Floquet exponent $\lambda_1$ and corresponding initial vector $\mathbf{a}^{(1)}(0)$ were obtained using algorithm (12.3*b*). The time integration starting with the initial condition $\mathbf{a}^{(1)}(0)$ was carried out using the Runge–Kutta–Nystrom algorithm. For larger values of $R^\delta$ as many as 34 Galerkin terms ($N = 34$) were used.

## 13. Results and conclusions

The single most important Stokes layer corresponds to $\beta = \infty$ since it is this one that plays the role of a viscous boundary-layer correction in oscillatory flows. However, Galerkin's method only seems justified for $\beta < \infty$, so that a compromise must be made between good approximation of the Stokes layer on one hand and the convergence of Galerkin's method on the other. The value $\beta = 8$ was chosen. This is consistent with the energy-theory results of von Kerczek & Davis (1972), who found that the critical Reynolds numbers of that theory for $\beta = 8$ and $\beta = \infty$ were within 1 % of each other. However, it must be kept in mind that no finite value of $\beta$ approximates the case $\beta = \infty$ for all values of $\alpha$ since as $\alpha \to 0$, the $\beta < \infty$ problems have non-trivial solutions of the disturbance equation with finite values of $\alpha R^\delta$ (see (8.6)) while for $\beta = \infty$, $\alpha R^\delta \to \infty$ as $\alpha \to 0$. Clearly, long enough disturbance waves feel the influence of a second wall finitely placed.

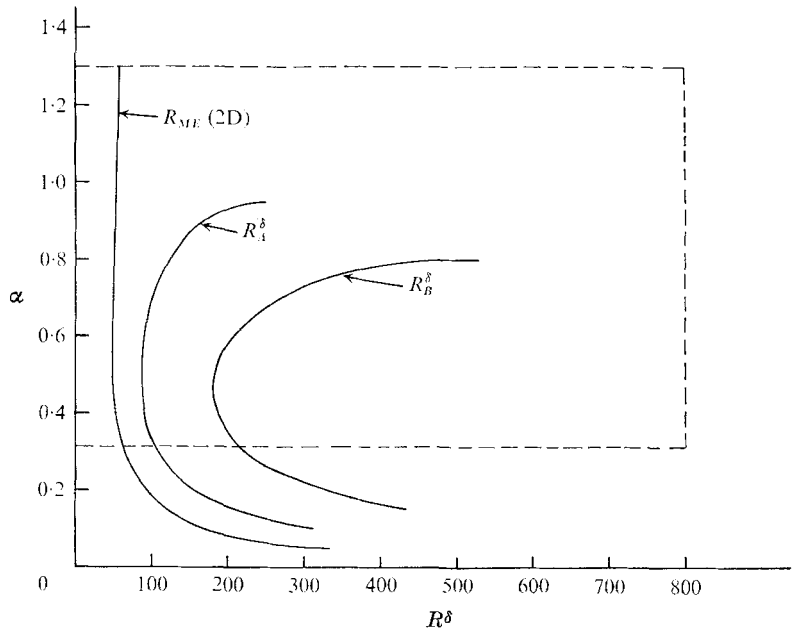


FIGURE 2. The energy limit $R^\delta_{ME}$ and quasi-static neutral curves for the finite Stokes layer; $\beta = 8{\cdot}0$. The dotted rectangle encloses the region of detailed calculations of absolute stability for the full time-dependent problem. When $\alpha = 0$, there is also absolute stability.

Figure 2 is used to enter the neutral-curve information obtained. The lowest curve in figure 2 corresponds to $R^\delta = R^\delta_{ME}(2\mathrm{D})$, the mean energy limit of Davis & von Kerczek (1973). Below this curve two-dimensional disturbances of arbitrary amplitude decay to zero exponentially when averaged over a cycle of the basic state. The minimum value of $R^\delta$ on this curve is 47·1. It is only above this curve in the $\alpha$, $R^\delta$ plane that instabilities may exist.

In comparison with the full time-dependent linear theory, the relative ease of calculation under a quasi-static assumption is enormous. This is one of the reasons for its popularity. Two such theories were applied to the Stokes layer for $\beta = 8$. Quasi-static theory $A$ seeks to make the most dangerous frozen profile (near $t_0 = \frac{1}{2}\pi$) neutral. This neutral curve was computed and labelled $R^\delta_A$ in figure 2. The minimum of this curve occurs near $\alpha = 0{\cdot}5$ and is $\min_\alpha R^\delta_A = 86{\cdot}0$. Quasi-static theory $B$ allows growth at some instants $t_0$ but seeks a zero value of the growth rates averaged over a cycle of the Stokes layer. This neutral curve was computed and labelled $R^\delta_B$ in figure 2. The minimum of this curve occurs near $\alpha = 0{\cdot}5$ and is $\min_\alpha R^\delta_B = 182$.

The quasi-static assumption accomplishes two simplifications. It allows the reduction of the governing disturbance equation (5.2) from a partial differential equation to an ordinary differential equation (5.3), the Orr–Sommerfeld equation. Simultaneously, it makes the inviscid limit well-behaved, so that inflexional instabilities of the frozen profiles are expected. Hence, the low critical values of $R^\delta$ under the theories are natural.

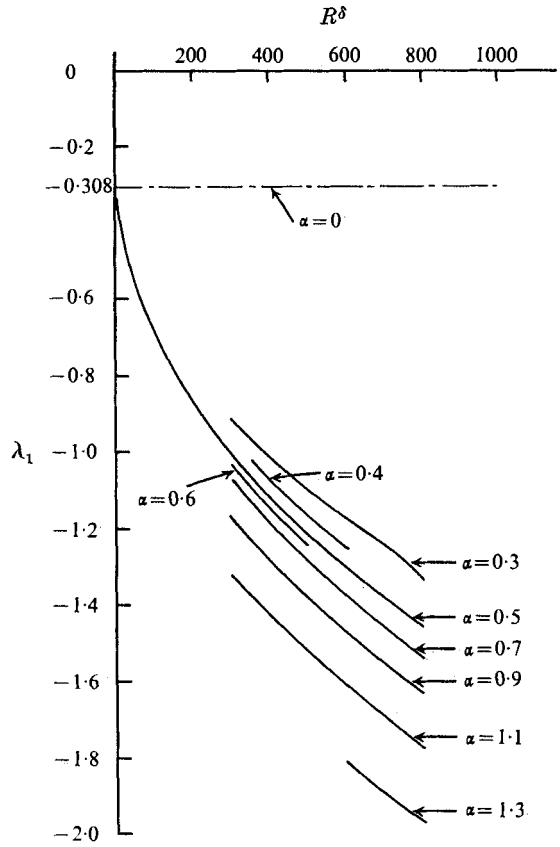


FIGURE 3. The principal Floquet exponents $\lambda_1$ *vs.* $R^\delta$ for $\beta = 8{\cdot}0$ and various $\alpha$.

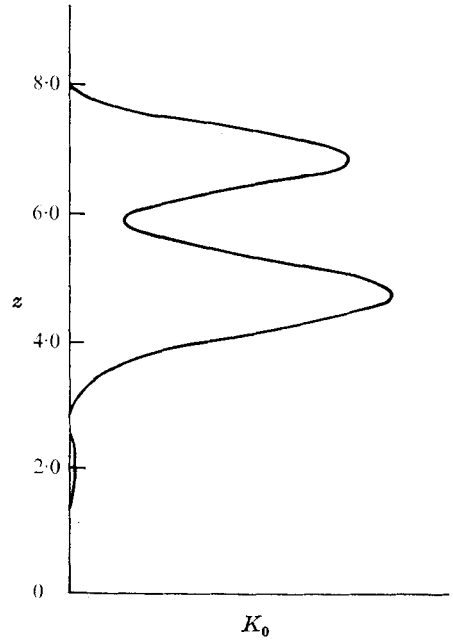


FIGURE 4. The initial ($t = 0$) energy distribution $K_0$ of the principal disturbance mode for $\alpha = 0{\cdot}5$, $\beta = 8{\cdot}0$ and $R^\delta = 600$.

| $R^\delta$ \ $\alpha$ | 0·3 | 0·4 | 0·5 | 0·6 | 0·7 | 0·9 | 1·1 | 1·3 |
|---|---|---|---|---|---|---|---|---|
| 0 | — | — | −0·327 | — | — | — | — | — |
| 50·0 | — | — | −0·551 | — | — | — | — | — |
| 100·0 | — | — | −0·682 | — | — | — | — | — |
| 160·0 | — | — | −0·799 | — | — | — | — | — |
| 185·0 | — | — | −0·841 | — | — | — | — | — |
| 225·0 | — | — | −0·900 | — | — | — | — | — |
| 300·0 | −0·915 | — | −1·01 | −1·03 | — | −1·17 | −1·32 | — |
| 350·0 | — | −1·02 | — | — | — | — | — | — |
| 400·0 | −1·02 | — | −1·12 | −1·15 | −1·19 | — | — | — |
| 425·0 | — | −1·10 | −1·14 | — | — | — | — | — |
| 450·0 | — | — | — | — | — | −1·34 | — | — |
| 500·0 | −1·10 | −1·17 | −1·21 | −1·29 | −1·29 | — | — | — |
| 585·0 | — | — | −1·29 | — | — | — | — | — |
| 600·0 | −1·17 | −1·26 | −1·30 | — | −1·38 | −1·48 | −1·62 | −1·82 |
| 700·0 | −1·25 | — | −1·39 | — | −1·46 | −1·56 | — | — |
| 800·0 | −1·34 | — | −1·46 | — | −1·54 | −1·64 | −1·78 | −1·97 |

TABLE 2. The principal Floquet exponent $\lambda_1$ ($\beta = 8$) for various $\alpha$ and $R^\delta$.

The full time-dependent problem (9.3) was then integrated for $\beta = 8$. The principal Floquet exponent $\lambda_1$ turns out to be real in each case. These values of $\lambda_1$ are given in table 2 and plotted *vs.* $R^\delta$ in figure 3 for various $\alpha$. The range $0{\cdot}3 \leqslant \alpha \leqslant 1{\cdot}3$, $0 \leqslant R^\delta \leqslant 800$ was investigated and is indicated in figure 2 by the rectangle. The Floquet exponents for $\alpha < 0{\cdot}3$ were not calculated because the finite Stokes layer with $\beta = 8{\cdot}0$ does not adequately simulate the Stokes layer ($\beta = \infty$) in this range of $\alpha$. A rough estimate of the lower limit on $\alpha$ for which $\beta = 8$ adequately simulates $\beta = \infty$ was made with the quasi-static theory *A*. At $\alpha = 0{\cdot}2$ the difference between the quasi-static critical $R^\delta$ at $\beta = 8$ and $\beta = \infty$ is about 10% (von Kerczek 1973). However, the Floquet exponent at $\alpha = 0$ is obtained exactly, equation (8.6), and is shown as the dotted line in figure 3. These modes are, likewise, strongly stable, so that stability in the range $0 < \alpha < 0{\cdot}3$ is expected, as well. For certain cases the principal eigenfunction was then examined by obtaining its appropriate initial value. The initial ($t = 0$) kinetic energy distribution

$$K_0(z) = \frac{\alpha}{2\pi}\int_0^{2\pi/\alpha} (u^2+v^2)_{t=0}\,dx$$

is plotted in figure 4. Note that the region $z \leqslant 2$ occupied by the boundary layer is relatively inactive. The principal eigenfunction is then calculated (see table 1 for a typical one) and the energy balance (11.6 *d*) examined. Each term was calculated and inserted in this balance as a consistency check. This equation yielded an identity to eight significant figures for each case tested. The disturbance kinetic energy $K$ is plotted *vs.* $t$ in figure 5 for $\alpha = 0{\cdot}5$ and $R^\delta = 100$, 185, 400 and 600. Notice the more rapid decay for increasing $R^\delta$. Table 1 gives the initial vector $\mathbf{a}^{(1)}(0)$ for the case $\beta = 8{\cdot}0$, $\alpha = 0{\cdot}5$, $R^\delta = 600$ and $N = 26$. Finally, the production term given by (11.7) was calculated for $\alpha = 0{\cdot}5$ and $R^\delta = 185$ and 600. These are shown in figure 6.

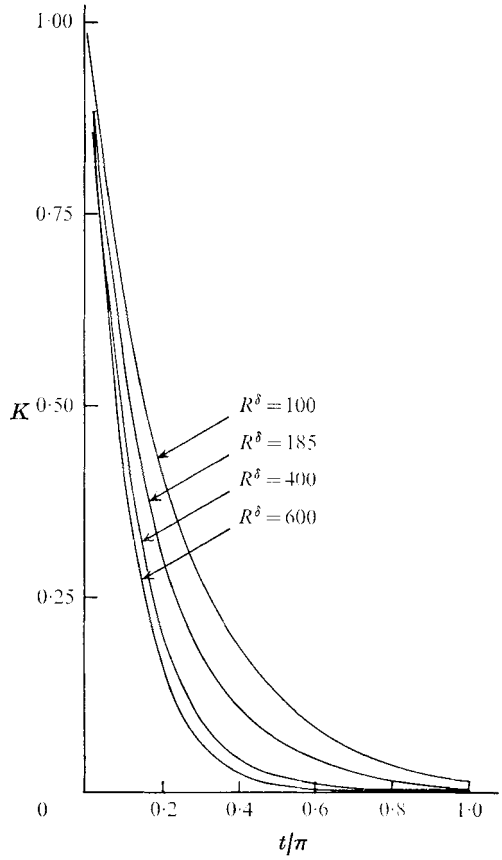


FIGURE 5. The total kinetic energy $K$ of the principal disturbance mode *vs.* $t$ for $\beta = 8{\cdot}0$ and $\alpha = 0{\cdot}5$.

Within the rectangle of figure 2, $0{\cdot}3 \leqslant \alpha \leqslant 1{\cdot}3$, $0 \leqslant R^\delta \leqslant 800$, the full time-dependent linear theory predicts *absolute stability* with $\lambda_1$ a monotone decreasing function of $R^\delta$ for fixed $\alpha$ and for $\beta = 8$. That is, *as the Reynolds number is increased the most dangerous mode of a given wavenumber becomes more stable.* Larger Reynolds numbers allow a greater transfer of disturbance energy *to* the mean flow. This is illustrated in figure 5, where the disturbance kinetic energy $K$ is shown as a function of time for various $R^\delta$. $K$ decreases more rapidly for larger $R^\delta$. The small positive region of the production term reflects the positive region in the principal eigenfunction at $t = 0$ which survives the time integration owing to the rapid decay of the solutions. Thus, the finite Stokes layer for $\beta = 8$ seems more stable than the motionless state (also see figure 4).

The last group of calculations made was for $\beta = 12$, 16 and 20 for $\alpha = 0{\cdot}5$. The eigenvalue $\lambda_1$ is given in table 3 and is shown in figure 7 along with its companion at $R^\delta = 0$. As $\beta$ increases, $\lambda_1$ approaches the $R^\delta = 0$ curve but always remains below it. This gives further validity to the notion that a disturbance of a given wavenumber of the Stokes layer is more stable than that of the motionless state. As $\beta \to \infty$, the basic state approaches a shear-layer discontinuity at $z = 0$. A disturbance of the basic state is most dangerous in the motionless fluid and as $\beta$

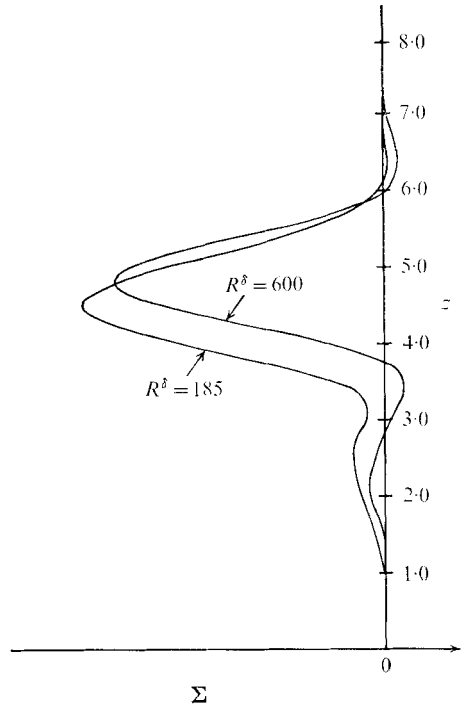


FIGURE 6. The time-averaged production term $\Sigma$ *vs.* $z$ for $\beta = 8{\cdot}0$ and $\alpha = 0{\cdot}5$.

increases, the motionless fluid occupies more and more of the region. Hence, the presence of the walls constrains the disturbance less and less. The limiting case is $R^\delta = 0$, where the walls are effectively farthest apart. This suggests that, although no calculations were done for $R^\delta > 800$, the Stokes layer may, in fact, be stable for all $R^\delta$ within the realm of linear theory.

However, finite amplitude (subcritical) instabilities are certainly possible and are suggested by the experiments of Li (1954) and Sergeev (1966), who obtained experimental critical values of $R^\delta$ for transition to turbulence of 566 and 500, $3 \leqslant \beta \leqslant 30$, respectively. Of the two sets Sergeev's experiments are much more extensive. In his nearly 100 runs he measured the critical Reynolds numbers both by observing marker particles and by measuring the average power per cycle needed to drive the bellows.

These values seem consistent with the results of this paper in that they show that the Stokes layer is remarkably stable. A Reynolds number $R^\delta = 500$ is an enormous value for an experiment where the induced motion is generated by a wall oscillating in its own plane. If the *displacement* of the wall is given by $X_0 \sin \omega t$, then $U_0 = \omega X_0$ and $R^\delta$ is given by

$$R^\delta = U_0 \delta/\nu = 2X_0/\delta. \tag{13.1}$$

A Reynolds number of 500 implies a wall displacement amplitude of 250 times $\delta$. This would be extremely large if one wanted to make $\delta$ large enough to take careful measurements within the boundary layer.

| $\beta$ | $R^\delta$ | $\lambda_1$ |
|---|---|---|
| 12 | 600 | −0·374 |
| 16 | 300 | −0·196 |
| 16 | 600 | −0·208 |
| 20 | 600 | −0·163 |

TABLE 3. The principal Floquet exponent $\lambda_1$ for various $\beta$ and $R^\delta$ and $\alpha = 0{\cdot}5$.

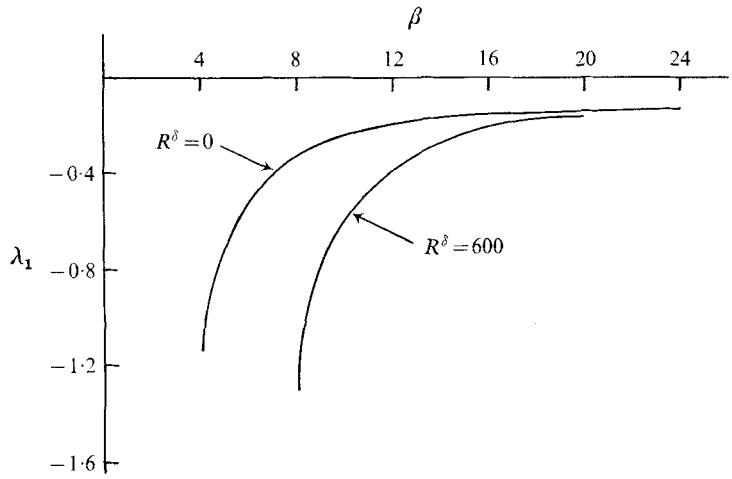


FIGURE 7. The principal Floquet exponents $\lambda_1$ *vs.* $\beta$ for $\alpha = 0{\cdot}5$.

The significantly lower critical Reynolds numbers found by Vincent (1957) and Collins (1963) indicate that the stability of modified Stokes layers on the bottom of water channels with travelling surface waves is strongly influenced by the normal component of velocity and/or the steady drift in the basic state.

Why do the time-dependent results differ so much from the quasi-static theories? The Stokes layer is a flow with a zero mean. Hence, the only reasonable time scale is $\omega^{-1}$. A flow with a non-zero mean has a convective time scale available as well. Since $\omega^{-1}$ was used for the time scale in the present analysis, the Floquet exponents computed are non-dimensional measures of the decay (or growth) rate of a disturbance measured against the scale of variation of the basic state. The numerical results show that $\lambda_1 = O(1)$. The quasi-static assumption, however, assumes that disturbances vary much faster than $\omega^{-1}$, so that it could only be valid if $|\lambda_1| \gg 1$. Hence, the results show that there is only a single time scale in the Stokes-layer stability problem and quasi-steadiness is not a good approximation. The same reasoning could be posed in more familiar terms. A steady basic state with a point of inflexion is expected to have $O(1)$ growth rates for Reynolds number $R = \infty$. As $R$ is lowered from infinity, the associated growth rate could still be $O(1)$. If the basic state were 'slowly varying' in time, one would again expect a sizeable growth rate. However, the Stokes layer has an $O(1)$ basic time variation. Hence, inflexion points propagate away before instabilities can grow locally. The above results and reasoning should hold true for general time-dependent stability problems as well. The quasi-static approach

must be justified by scale analysis as has been done by Shen (1961), and it seems clear that the worst place to apply it is at the neutral curve, where disturbances neither grow nor decay.

Rosenblat (1968) discusses a new mechanism of inviscid instability whose necessary condition is a velocity–vorticity phase shift. This criterion cannot be evaluated here for two reasons. First, the Stokes layers have no well-defined inviscid limit. Second, Rosenblat's condition is necessary for instability, and no instability at all is found here for Stokes layers.

S. H. D. would like to thank the National Science Foundation, Applied Mathematics Division for support under grants GP 17562 and GP 33933X. The facilities of the National Center for Atmospheric Research, supported by the National Science Foundation, provided the bulk of the computing facilities necessary for the calculations. Mr H. P. F. Nguyen provided us with his Fortran IV version of the LR algorithm.

## REFERENCES

CODDINGTON, E. A. & LEVINSON, N. 1955 *Theory of Ordinary Differential Equations.* McGraw-Hill.

COLLINS, J. I. 1963 *J. Geophys. Res.* **18**, 6007.

CONRAD, P. W. & CRIMINALE, W. O. 1965 *Z. angew. Math. Phys.* **16**, 233.

DAVIS, S. H. 1971 *Proc. IUTAM Symp. on Unsteady Boundary Layers*, Quebec.

DAVIS, S. H. & VON KERCZEK, C. 1973 *Arch. Rat. Mech. Anal.* **52**, 112.

DOLPH, C. L. & LEWIS, D. C. 1958 *Quart. Appl. Math.* **26**, 97.

DONNELLY, R. J. 1964 *Proc. Roy. Soc.* A **281**, 130.

DRAZIN, P. G. & HOWARD, L. N. 1966 *Adv. in Appl. Mech.* **9**, 1.

FFOWCS WILLIAMS, J. E., ROSENBLAT, S. & STUART, J. T. 1969 *J. Fluid Mech.* **39**, 547.

GALLAGHER, A. P. & MERCER, A. McD. 1962 *J. Fluid Mech.* **13**, 91.

GROSCH, C. E. & SALWEN, H. 1968 *J. Fluid Mech.* **34**, 177.

ISAACSON, E. & KELLER, H. B. 1966 *Analysis of Numerical Methods.* Wiley.

KERCZEK, C. VON 1973 Ph.D. thesis, Department of Mechanics, Johns Hopkins University.

KERCZEK, C. VON & DAVIS, S. H. 1972 *Studies in Appl. Math.* **51**, 239.

KERCZEK, C. VON & DAVIS, S. H. 1974 Pending publication.

LAMBERT, J. & MITCHELL, A. 1962 *Z. angew. Math. Phys.* **13**, 223.

LAPIDUS, L. & SEINFELD, J. H. 1971 *Numerical Solutions of Ordinary Differential Equations.* Academic.

LI, H. 1954 *Beach Erosion Bd., U.S. Army Corps Eng., Washington, Tech. Mem.* no. 47.

LONGUET-HIGGINS, M. S. 1953 *Phil. Trans.* A **245**, 535.

OBREMSKI, H. J. & MORKOVIN, M. V. 1969 *A.I.A.A. J.* **7**, 1298.

O'BRIEN, V. & LOGAN, F. E. 1965 *Johns Hopkins University, Appl. Physics Lab. Tech. Mem.* TG-658.

RILEY, N. 1966 *Quart. J. Mech. Appl. Math.* **19**, 461.

ROSENBLAT, S. 1968 *J. Fluid Mech.* **33**, 321.

SERGEEV, S. I. 1966 *Mekh. Zh. i Gaza*, **1**, 168. (Trans. *Sov. Fluid Dyn.*)

SHEN, S. F. 1961 *J. Aero. Sci.* **28**, 397.

SQUIRE, H. B. 1933 *Proc. Roy. Soc.* A **142**, 621.

VINCENT, G. E. 1957 *Proc. Conf. Coast. Eng.* **6**. University of Florida.

WANG, C.-Y. 1965 *J. Sound Vib.* **2**, 257.

WILKINSON, J. H. & REINSCH, C. 1971 *Linear Algebra.* Springer.